Identifying and characterizing yield limiting factors in paddy rice using remote sensing yield maps

Yi-Ping Wang · Shou-Hung Chen · Kuo-Wei Chang · Yuan Shen

Abstract Identification and characterization of yield limiting factors based on multi-year yield maps is important for delineating field management zones. Multi-year yield maps were derived from satellite images of a paddy-rice (*Oryza sativa* L.) study site with a conventional two-cropping system in central Taiwan. Spatiotemporal yield-trend maps with consistently high, average and low yields, and inconsistent yield areas were delineated based on temporal variation and the means of the normalized yields on a per pixel basis. Soil and plant samples were collected and grouped for statistical analysis based on the derived yield-trend maps. Comparison of soil properties and rice yield components among yield classes indicated that differences in leaching loss of basal and top-dressed N fertilizers were the likely limiting factor affecting the spatial variation of yield within the study site.

Keywords Environmental pollution · N fertilization · Soil management

Abbreviations

ANOVA	Analysis of variance
CV	Coefficient of variation
EC	Electrical conductivity
GRN	Green
H	Consistent-high
L	Consistent-low
LAI	Leaf area index

Y.-P. Wang · Y. Shen (✉)
Department of Soil and Environmental Sciences, National Chung-Hsing University, Taichung, Taiwan, ROC
e-mail: yshen@nchu.edu.tw

S.-H. Chen
Department of Geography, Chinese Cultural University, Taipei, Taiwan, ROC

K.-W. Chang
Department of Leisure and Recreation Studies, Aletheia University, Tainan, Taiwan, ROC

M	Consistent-average
RED	Red
N	Nitrogen
NDVI	Normalized difference vegetation index
NIR	Near infrared
p-value	Statistical significance
SSCM	Site-specific soil and crop management
SD	Standard deviation
SPOT	Satellite Pour l'Observation de la Terre
SY	Standardized yield
V	Inconsistent

Introduction

Site-specific soil and crop management (SSCM), also known as precision agriculture, is a farming system that considers spatial and temporal variability in soil properties and crop productivity (Mulla and Schepers 1997). This farming system is expected to improve the efficiency and efficacy of fertilizers, which in turn may reduce environmental pollution due to excessive fertilizer application (Powers et al. 2000; Cassman et al. 2002; Ferguson et al. 2002; Hong et al. 2006). The concept of SSCM promotes the delineation of management zones, i.e., subfield regions that are similar based on certain quantitative measures and the application of appropriate management practices.

Various information sources have been used to delineate SSCM management zones, e.g., soil survey maps (Steinwand et al. 1996), soil zones based on topography (Franzen et al. 2000),yield maps created by yield monitors (Birrell et al. 1993), bulk soil apparent electrical conductivity (Fraisse et al. 2001; Franzen and Nanna 2002; Kitchen et al. 2003; Schepers et al. 2004), soil survey boundaries modified by aerial photos (Carr et al. 1991), and the management experiences of a producer in combination with aerial photographs (Fleming et al. 2000, 2004). However, crop yields are affected by a complex combination of dynamic interactions between biotic, soil and climatic factors. The temporal instability of delineated management zones is problematic when characterizing yield-soil relationships and making management decisions (Jaynes and Colvin 1997; Machado et al. 2002; Fraisse et al. 2001).

Several researchers have suggested that the production of multi-year yield maps may be essential for optimized site-specific crop management decision making (Pierce et al. 1997; McBratney et al. 2000; Tiffany et al. 2000; Cox and Gerard 2007). The number of years of data that are required to represent the range of possible yield outcomes for each crop grown on a field is unique and dependent on stochastic interactions of the crop, climate, soil and landscape (Lamb et al. 1997; Dobermann et al. 2003; Schepers et al. 2004; Boydell and McBratney 2002). However, multi-year yield maps may not be available for many fields, which imposes a practical limitation on the application of SSCM.

Remote sensing has long been recognized as a useful tool for acquiring crop information (Frazier et al. 1997; Hatfield et al. 2008). Leaf pigments, particularly chlorophyll, absorb mainly the blue and red portions of incoming solar energy spectrum, which can result in very low canopy reflectance in the visible region (Blackmer et al. 1996; Hansen and Schjoerring 2003). Increased reflectance in the near infrared (NIR) region is related to increased crop biomass and leaf area index (LAI) (Guyot 1990; Broge and Leblanc 2000;

Thenkabail et al. 2000; Thenkabail 2002). Thus, changes in the canopy reflectance spectrum in the visible and near infrared regions should be associated with crop yield (Wiegand et al. 1994; Aparicio et al. 2000). A rice yield forecasting model was proposed by Chang et al. (2005) and modified by Wang et al. (2010), which used ratios of reflectance in the NIR band to the red band (NIR/RED) and the NIR band to the green band (NIR/GRN) to estimate the effects of LAI and N status of plants, respectively. The model has been used successfully to estimate rice yields at the field scale based on surface reflectance data retrieved from SPOT (Satellite Pour l'Observation de la Terre) multispectral images (Wang et al. 2010). Therefore, the huge database of available satellite images could be a valuable source of information for producing proxy yield maps that can be used to delineate management zones.

The excessive application of fertilizers by farmers has already produced serious environmental pollution problems in Taiwan. As a pilot SSCM study for paddy-rice, the major cultivated crop in Taiwan, the objectives of this study were to characterize the spatial variability in paddy-rice vigor using satellite images as a proxy for a yield map and then use plant and soil sample data to postulate cause-and-effect relationships so that spatial management practices could be implemented.

Materials and methods

Site description

The selected paddy-rice site was located in central Taiwan (24°18′40″ N, 120°38′30″ E) and was bounded by the Tachai River with a terrace measuring about 50 m in height. The site contained 435 fields and covered an area of ∼100 ha with an average field size of ∼0.2 ha (Fig. 1). This site was originally part of the Tachai River. After the completion of a protective embankment in 1985, soil was brought in from a nearby area and mixed with river sand before paddy-rice production commenced. The soils in this experimental site were classified as Fluvaquentic Dystrochrept with a coarse texture and very shallow depth (generally <0.4 m).

Paddy-rice (*Oryza sativa* L.), semi-dwarf *japonica* type cultivars Taikeng 8, Taikeng 11 and Taikeng 16 were grown at the site during the study period (2006–2009). These cultivars all have stable and high yielding traits, although they differ in their susceptibility to plant diseases. A conventional two-season cropping system was practiced at the site. Transplantation generally began in early February and again in late July, with harvesting in late June and late November of the first and the second crop season, respectively.

Fields were generally prepared and flooded seven days before transplantation. Floodwater depth of 0.05–0.1 m was maintained for about 50 days during the first crop season (40 days in the second crop season) before draining and followed by intermittent irrigation (1–2 days flooding at a depth of about 0.01–0.02 m every 2 weeks) until maturity. The average fertilizer application rates by farmers per crop season were 206 kg N ha^{-1}, 101 kg P_2O_5 ha^{-1}, and 95 kg K_2O ha^{-1}, which far exceeded local recommendations for sandy soils (i.e., 140 kg N ha^{-1}, 40 kg P_2O_5 ha^{-1}, and 40 kg K_2O ha^{-1}). Insects, diseases, and weeds were controlled by regularly spraying pesticides throughout the growth period to avoid yield loss. The apparent over-application of fertilizers is a potential source of pollution that could affect the ecology of the downstream Tachai River estuary.
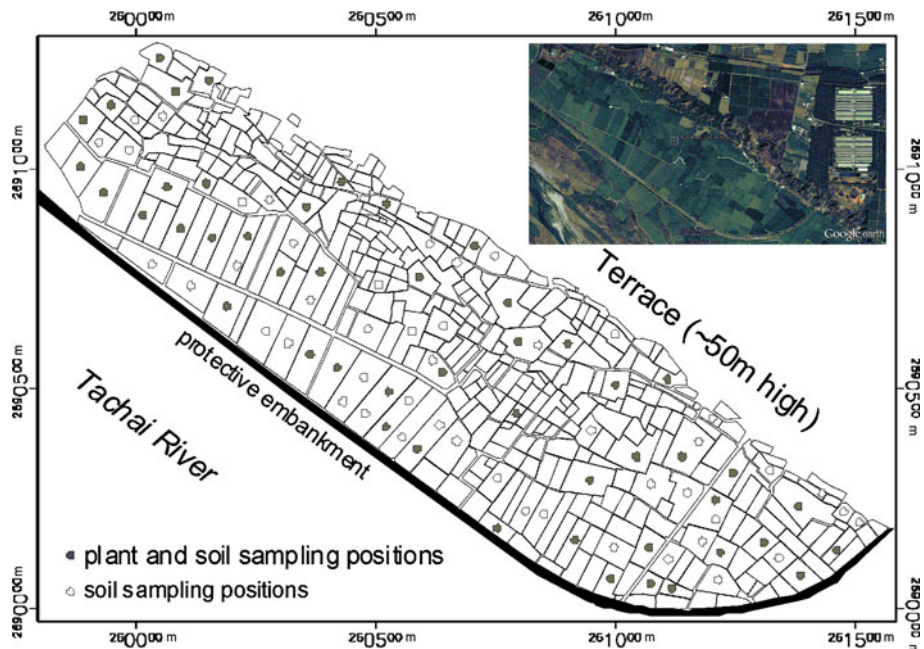
Fig. 1 Schematic diagram, using Universal Transverse Mercator (UTM) coordinates, indicating the field borders and plant and soil sampling positions within the study site. A Google Earth image is also attached to aid the understanding of the illustration and the environment

Table 1 Imaging conditions for SPOT images used in this study and atmospheric settings for surface reflectance retrieval by FLAASH

Dates	Sensors	Imaging angles (°)		Atmospheric settings	
		Incidence	Orientation	Aerosol model	Visibility (km)
2006/09/24	SPOT4	−11.0	12.6	Urban	18
2007/05/07	SPOT4	−13.8	8.8	Maritime	17
2007/09/30	SPOT4	−25.1	8.1	Maritime	11
2008/04/26	SPOT2	−14.1	8.9	Maritime	15
2008/10/12	SPOT4	29.2	11.3	Maritime	20
2009/05/04	SPOT4	−14.1	8.8	Rural	15

Yield map retrieval from satellite images

Six Level-3 SPOT images obtained between panicle initiation and the heading stages in each crop season were purchased from the Center for Space and Remote Sensing Research, National Central University, Taiwan (Table 1). Atmospheric correction of these images was conducted using FLAASH (Fast Line-of-sight Atmospheric Analysis of Spectral Hypercubes, Version 4.1, ITT Visual Information Solutions, Boulder, CO, USA) as described by Wang et al. (2010).

Rice yields during the first and second crop season were estimated in each year on a per pixel basis (20 × 20 m) using the models described by Wang et al. (2010) for the retrieved surface reflectance in the GRN, RED and NIR bands.

$$1^{st}\text{crop Y } \left(\text{t ha}^{-1}\right) = 1.96(\text{NIR/GRN}) - 0.658(\text{NIR/RED}) - 1.50 \qquad (1a)$$

$$2^{nd}\text{crop Y } \left(\text{t ha}^{-1}\right) = 1.96(\text{NIR/GRN}) - 0.729(\text{NIR/RED}) - 1.64 \qquad (1b)$$

The NIR/GRN ratio represents the plant N sufficiency, which is driven by the chlorophyll content and the LAI, whereas the NIR/RED ratio relates mainly to the LAI (Hatfield et al. 2008). Grain yield should be closely related to net photosynthesis, so the yield estimate by Eq. (1) should increase with increasing NIR/GRN (accounting for gross photosynthesis) whereas it should decrease as NIR/RED (accounting for respiration loss) increased. Two sets of coefficients were required because of the reversal of the temperature and solar radiation environments in the first (from February to June) and second (from July to November) rice crop seasons in Taiwan. These relationships were applicable over a yield range of 2–12 t ha^{-1}.

Figure 2 illustrates the distribution of normalized difference vegetation index (NDVI) values for each pixel within the study site. Based on ∼400 paddy-rice canopy reflectance measurements which covered a wide yield range, Wang et al. (2010) indicated that NDVI values should be ≥0.79 for paddy fields at booting stages. Therefore, pixels that had NDVI values <0.79 were discarded because they might have been severely compromised by clouds, roads, set-aside fields and fields planted with other crops. The borders of each paddy field were <0.2 m wide, which was relatively smaller compared with the width (≥20 m) of each field, and they were generally obscured by the plant canopy after the maximum tillering stage. Thus, field borders would be expected to have little impact on canopy reflectance from the paddy canopy.

Yield classification and management zone delineation

The historical yield maps that were generated from the retrieved satellite images were then subjected to spatial and temporal trend analysis, as described by Blackmore (2000). To compare yield patterns across years and seasons, yield data of each location (y$_i$) were first

Fig. 2 Cumulative frequencies of pixel NDVI values within the study site for each year and crop season
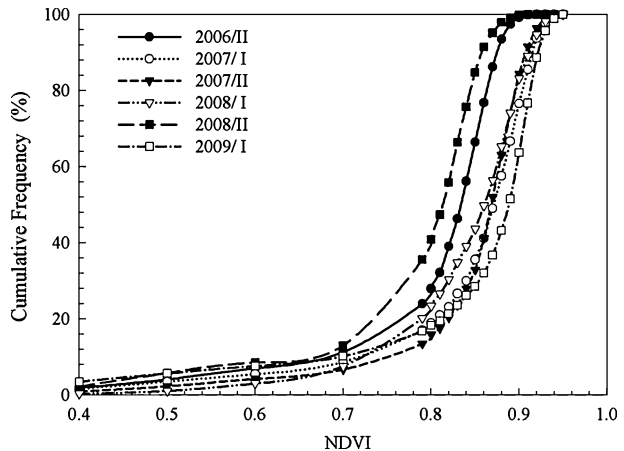
normalized (SY_i) by the average yield of all locations for each year and crop season ($\tilde{y}$) using Eq. (2).

$$SY_i = (y_i/\tilde{y}) \qquad (2)$$

Not all paddy-rice pixels had yield data available for all six crop seasons because of cloud cover and some fields were either planted with other crops or set-aside. Therefore, only pixels that had a complete yield dataset (i.e., six yield datasets) were considered as effective pixels and used in further analysis. For each effective pixel, the six normalized yield values were then averaged to create a mean normalized yield. The yield temporal variability for each pixel was determined by the coefficient of variation (CV). Pixels with a CV > 30 % were considered to be highly variable and classified as inconsistent (V) (Wollenhaupt et al. 1997). Since the normalized yield values of each particular year/season had a bell-shaped distribution, we further divided those consistent pixels (CV ≤ 30 %) into three yield classes based on the standard deviation (SD = 0.13) of all the normalized yield values. Thus, pixels with normalized yield values >1.13 were considered consistently high (H), values ≥0.87 and ≤1.13 were considered consistently average (M), and values <0.87 were considered consistently low (L). Using this classification, the majority of pixels were classified into the M class, but there were sufficient H and L class pixels (∼15 % each) for further statistical analysis.

Soil sampling and analysis

To relate the soil chemical and physical properties to yield classes, a total of 98 soil samples were collected after harvesting the second crop during 2007 and 2008 (Fig. 1). Fifty samples were initially collected in 2007 based on the yield classification map derived from a satellite image of the second crop season in 2006. An additional 48 samples were added in 2008 based on the updated yield classification maps from satellite images acquired in 2006–2008. The sampling locations were then spatially joined to the corresponding SY data, where we used the SY_i data with the center point closest to the soil sampling point to represent the yield at that sampling point. Of the 98 soil sampling positions, 79 were classified as consistent in the yield classification.

Each soil sample (0–0.15 m) consisted of three subsamples collected from a 5-m radius around the sampling point. Soil samples were air dried and grounded to pass through a 2-mm sieve. Soil pH and EC (electrical conductivity) were determined with a 1:1 soil water ratio, texture using the hydrometer method, total C and N using the dry combustion method and available P, K, Ca, Mg, Fe were extracted using the Mehlich No. 3 method (Klute 1986; Sparks 1996). Descriptive statistics for the analyzed soil properties are listed in Table 2.

Plant sampling and analysis

Plant data were collected during each crop season from 2007 at 50 selected sample sites where soil samples had also been taken (Fig. 1). At about 60 days after transplantation, chlorophyll meter readings were acquired at each sampling location using a Minolta SPAD-502 chlorophyll meter (Minolta Camera Co. Ltd., Osaka, Japan). Measurements were taken on the youngest collared leaf, midway between the stalk and the tip, and midway between the midrib and leaf margin (Balasubramanian et al. 2000). The chlorophyll meter readings acquired at each location were the averages of 5 hills (bundles of tillers that originated from transplanted seedlings).

Table 2 Descriptive statistics for the soil properties in the study site

Statistics	Sand %	Clay	pH	EC mS m^{-1}	C %	N	P mg kg^{-1}	K	Ca	Mg	Fe
Mean	66.1	13.4	5.0	7.5	1.52	0.17	54.5	70.4	625	206	655
SD	6.7	3.9	0.3	4.7	0.30	0.03	35.5	41.7	216	47	154
Minimum	53.9	6.8	4.2	2.0	0.83	0.09	7.4	27.7	257	104	311
Lower quartile	60.0	9.9	4.8	4.3	1.35	0.15	27.6	47.5	500	172	558
Median	65.2	13.1	5.0	6.0	1.52	0.17	47.5	57.4	608	210	645
Upper quartile	71.9	15.8	5.2	8.7	1.73	0.19	57.4	77.7	705	230	762
Maximum	81.9	23.1	5.6	22.5	2.32	0.23	181.8	303.5	1,795	364	1,121
Skewness	0.38	0.31	0.03	1.74	0.21	−0.25	0.97	3.34	2.39	0.30	0.49
Kurtosis	−0.61	−0.38	−0.08	3.00	−0.17	−0.35	0.74	14.5	10.9	0.44	0.37

Rice grain yields were the product of the plant's yield components: (1) the number of panicles (or effective tillers) per given area, (2) the number of spikelets (or grains) per panicle, (3) the fertility rate (percentage of filled grains) and (4) the weight of each grain (usually expressed as 1000-grain weight) (Yoshida 1981). Generally, an indication of the cause of problems during the season can often be determined from the yield components. At harvest, the number of panicles per hill, spikelets per panicle, fertilizer rate, and 1000-grain weight were determined from 5 hills of rice plants that were randomly selected and hand-harvested from each sampling location. The spikelet aerial density (spikelets m^{-2}) and grain yield (t ha^{-1}) were calculated using Eqs. (3) and (4).

$$\text{spikelet aerial density} = \text{panicles per hill} \times \text{spikelets per panicle} \times \text{planting density} \tag{3}$$

$$\text{grain yield} = A \times \text{spikelet aerialdensity} \times \text{fertility rate} \times \text{1000-grain weight} \tag{4}$$

where A is the unit conversion factor from grams per square meter to tones per hectare.

To facilitate the identification of differences in the growth and yield components, the collected yield data were also divided into three classes based on the SD of the yield data for each year/crop season. Values within 0.7SD units on either side of the mean were considered average. Values more than 0.7SD units below and above the mean were in the low and high classes, respectively. The criterion of 0.7SD was selected to ensure that the high and low yield classes represented the upper and lower quartiles of the yield data, respectively. Otherwise, the number of data in the high and low yield classes would have been too small because the spread of yield data was concentrated around the mean.

Statistical analysis

Descriptive statistics of yield and soil data were calculated using the Descriptive module in STATISTICA (StatSoft, Inc., Tulsa, OK, USA). Correlations of yield data between different year/crop seasons were calculated using the Correlation matrices modules in STATISTICA. Duncan's mean separation test was used to relate soil properties to changes in the yield classification from the first crop season to the second crop season, and to

determine any significant differences in chlorophyll meter readings and yield components between yield classes in each year/crop season using the Breakdown and one-way ANOVA module of STATISTICA.

Results and discussion

Temporal changes in yields

During the study period, the median grain yield values ranged from 5.3 t ha^{-1} in 2008 to 6.5 t ha^{-1} in 2007 for the first crop season, and from 4.2 t ha^{-1} in 2007 to 5.4 t ha^{-1} in 2008 for the second crop season (Fig. 3). The averaged grain yields of the first and the second crop season were 5.9 t ha^{-1} and 5.0 t ha^{-1}, respectively. Yield differences between the two crop seasons are common in Taiwan because the climatic conditions are different in the first and second crop season (Hsieh and Liu 1979).

Yearly climatic conditions at the study site varied during the study period (Fig. 4). Air temperatures in the early growth stages (February) of the first crop season in 2008 were lower than the 4-year means, whereas solar irradiances during the period from trans-plantation to heading (August to early October) of the second crop season in 2007 were lower than the 4-year means due to more rainy days. These may have resulted in a lower than normal yield for the first crop season in 2008 and the second crop season in 2007 (Fig. 3).

Link et al. (2006) considered that a Pearson's correlation coefficient higher than 0.5 between crop seasons represented a high temporal stability yield pattern. Of the 1 681 pixels that had a consistent yield trend with data available for all six crop seasons, the correlation analysis indicated that correlations were low (<0.3 in most cases) between any particular pair of year/crop season combinations (Table 3). However, the correlations between a particular year/crop season with the averages of the other 5 year/crop seasons
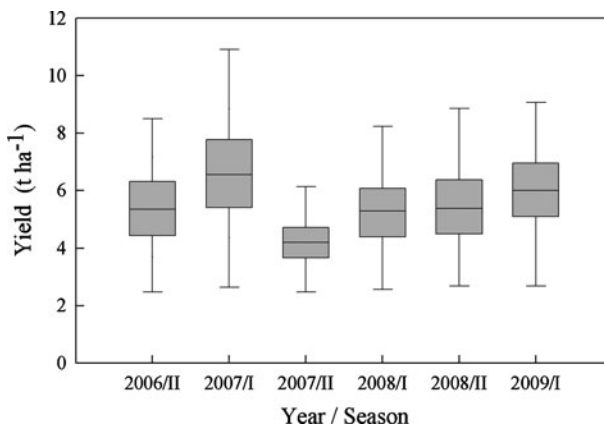
Fig. 3 Box-and-whisker plots of estimated yields for the 6-year/crop season at the study site. The caps at the end of each box indicate the extreme values (minimum and maximum), the box is defined by the lower and upper quartiles, while the line in the center of the box is the median. The length of the box indicates the interquartile range

Fig. 4 Changes in the 10-day **a** averaged air temperature and **b** accumulated solar irradiance from 2006 to 2009 at the study site. The means for 2006–2009 are also plotted
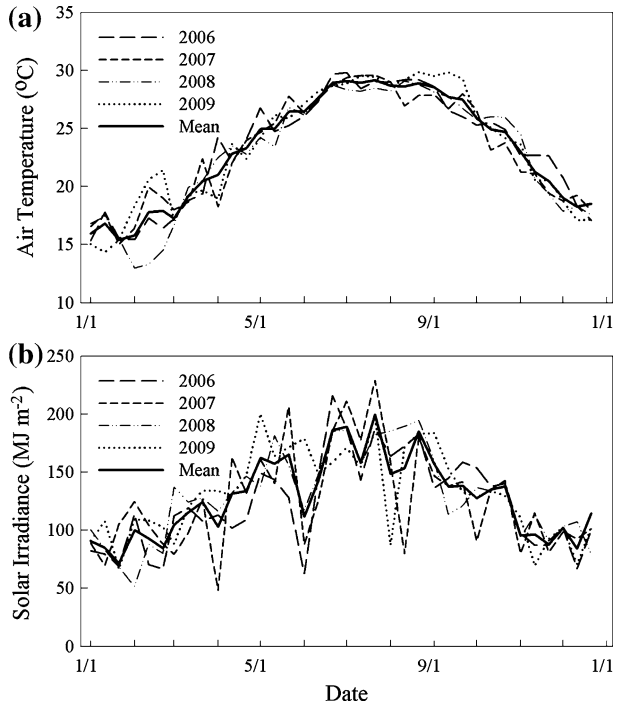
Table 3 Pearson correlation coefficients among the estimated yield of individual year/crop season (I: first crop season, II: second crop season), the averages of the first (Iavg) and the second (IIavg) crop season, and the overall average (I + IIavg)

Year/season	2006/II	2007/I	2007/II	2008/I	2008/II	2009/I
2007/I	0.28					
2007/II	0.23	0.26				
2008/I	0.25	0.42	0.18			
2008/II	0.09	0.03	0.17	0.10		
2009/I	0.22	0.35	0.30	0.28	0.29	
Iavg[a]	0.33	0.49	0.33	0.44	0.17	0.38
IIavg[a]	0.21	0.26	0.27	0.26	0.16	0.40
I + IIavg[a]	0.35	0.45	0.37	0.41	0.20	0.48

[a] Averages were computed by leaving out the correlated individual year/season

were better (0.35–0.48 in most cases). Little improvement in the correlation coefficients was observed when they were correlated with the averages of the corresponding crop season, particularly in the second crop season. These results suggested that the overall averaged normalized yield value was a better reference indicator of yield for each pixel.

The low correlations between yield map data for successive seasons did not necessarily indicate low intrinsic variation because the expression of limiting effects depended on factors such as weather and crop growth conditions that could differ between seasons. Consequently, yield map interpretation efforts have focused on identifying generalized

zones of low, average and high yield using the mean normalized yield value as the basis of yield classification.

Spatiotemporal distribution of the mean normalized yield

Of the 1 803 effective yield cells, 13.4 % were classified as consistently high, 65.2 % were classified as consistently average, 14.6 % were classified as consistently low, and 6.8 % were classified as inconsistent. The spatiotemporal yield map based on the mean normalized yield is shown in Fig. 5. To evaluate the temporal stability of the derived spatiotemporal yield map, statistics of the yield class changes from the derived spatiotemporal yield map for each crop season were compiled, as shown in Table 4. In most cases, over half of the pixels retained the same yield classification in a different year/season for each yield class. Downgrades from class H and upgrades from class L were generally within one level. Only several pixels (<15 out of 1 681 in most cases) had yield class changes greater than one level. Therefore, the derived spatiotemporal yield map may be considered to be temporally stable.

Questionnaires to local farmers within the study site revealed that management practices, such as planting date, irrigation, fertilization rate and timing were all very similar (data not shown) and there was no apparent occurrence of plant diseases due to regular pest and disease controls. Therefore, indigenous soil factors should be the main factors contributing to the spatiotemporal distribution observed.

Soil differences among yield classes

Duncan's mean separation tests were used to determine if differences existed in the soil properties among yield classes. Results indicated that consistently low yielding areas had a significantly lower EC and available-K content when compared with consistently high yielding areas (Table 5). Other analyzed soil properties were not significantly different among yield classes. All fields experienced similar management practices for a long
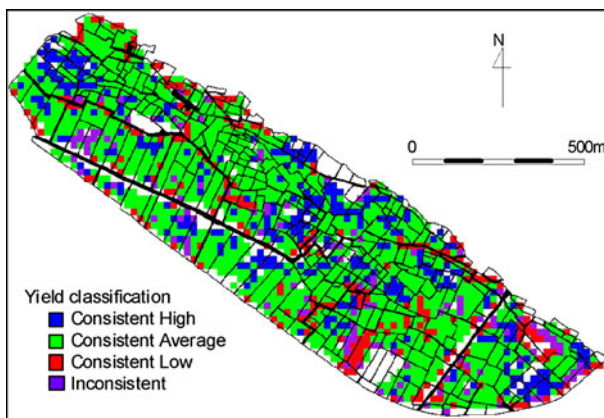
Fig. 5 Spatiotemporal yield trend map for the study site. Uncolored pixels were either severely contaminated by nearby non-paddy rice pixels or planted with other crops at least once in a crop season

Table 4 Percentage distribution of yield classes changes (YCC) from the derived spatiotemporal yield map for each yield class and individual year/crop season (I: first crop season; II: second crop season)

YCC[a]	Year/season					
	2006/II	2007/I	2007/II	2008/I	2008/II	2009/I
HH	61.2 (161)	70.7 (186)	49.0 (129)	58.2 (153)	46.8 (123)	65.8 (173)
HM	30.4 (80)	25.1 (66)	46.4 (122)	37.6 (99)	43.0 (113)	32.3 (85)
HL	8.4 (22)	4.2 (11)	4.6 (12)	4.2 (11)	10.2 (27)	1.9 (5)
MM	44.2 (520)	46.9 (551)	60.0 (705)	52.6 (618)	49.0 (577)	54.2 (637)
MH	28.8 (339)	25.4 (299)	20.9 (246)	23.1 (272)	25.8 (303)	24.0 (282)
ML	27.0 (317)	27.7 (326)	19.1 (225)	24.3 (286)	25.2 (296)	21.8 (257)
LL	74.4 (180)	75.6 (183)	67.4 (163)	70.7 (171)	58.3 (141)	70.3 (170)
LM	23.5 (57)	23.2 (56)	31.4 (76)	27.7 (67)	37.6 (91)	28.9 (70)
LH	2.1 (5)	1.2 (3)	1.2 (3)	1.6 (3)	4.1 (10)	0.8 (2)

Values shown in parentheses are the numbers of pixels

[a] The first letter represents the yield class in the derived spatiotemporal yield map; the second letter represents the yield class in each corresponding year/season

Table 5 Duncan's mean separation test ($p < 0.07$) for soil properties among yield classes (H: consistent-high, M: consistent-average, L: consistent-low)

Yield class	Sample number	Sand %	Clay	pH	EC mS m^{-1}	C %	N	P	K mg kg^{-1}	Ca	Mg	Fe
H	15	63.6	14.5	4.9	9.0 a	1.62	0.18	74.2	89.4 a	744 a	192	657
M	51	66.5	12.9	5.0	7.5 ab	1.54	0.17	49.7	67.2 ab	599 b	208	674
L	13	66.8	13.6	5.0	6.0 b	1.46	0.17	44.0	61.4 b	632 ab	203	604

period, so changes in the magnitude of EC values might be an indication of the heterogeneity of leaching loss within the study site.

Drought stress should not have occurred because of frequent irrigation. The soil pH values were neither basic nor very different among yield classes, whereas the EC values were significantly lower in consistently low yielding areas. The soils in the study site were very shallow and coarse in texture, so we suspected that leaching loss might be the dominant factor contributing to the observed spatial distribution of the mean standardized yield.

Yield component analysis

Duncan's mean separation tests were conducted to identify differences in yield components and chlorophyll meter readings among yield classes (Table 6). The results indicated that yield classes significantly aligned with aerial spikelet density during the year and crop season studied. High yield locations had a higher aerial spikelet density. The alignments of yield classes with fertility rate and 1000-grain weight were not as apparent as the aerial spikelet density. However, the low yielding locations generally had a lower fertility rates and 1000-grain weights.

The amount of N uptake at different growth stages strongly affected the formation of the respective yield components (De Datta 1981; Mae 1997). The N absorbed during the

Table 6 Duncan's mean separation test ($p < 0.05$) for chlorophyll meter readings (SPAD value) at the tillering stage and the analyzed yield components among yield classes in the corresponding year/crop season (I: first crop season; II: second crop season)

Yield class	SPAD value	Spikelet density m^{-2}	Fertility rate %	1000-grain weight g	Grain yield t ha^{-1}
2007/I					
High	40.1	44141a	92.9a	23.8a	9.7a
Average	39.7	32000b	90.2ab	22.8a	6.5b
Low	39.1	23719c	88.3b	20.9b	4.3c
2007/II					
High	38.1	35569a	80.5	24.4a	6.9a
Average	39.5	28334b	76.5	22.3b	4.7b
Low	39.1	19681c	73.6	20.8b	2.9c
2008/I					
High	40.5	44931a	94.0a	21.8	9.1a
Average	39.0	32166b	91.8ab	20.9	6.3b
Low	40.6	27203c	88.0b	19.8	4.6c
2008/II					
High	38.5	29441a	92.2a	23.0a	6.2a
Average	38.2	21401b	92.6a	22.1a	4.3b
Low	38.9	19695b	87.5b	18.6b	3.2c
2009/I					
High	NA[a]	46805a	87.4	23.2a	9.3a
Average	NA[a]	40530b	88.2	20.6b	7.2b
Low	NA[a]	28539c	82.9	21.4a	4.9c

[a] Data not available

vegetative stage (from transplanting to tillering) promotes early growth of plants and increases the number of tillers. The amount of N absorbed during the early phase of panicle formation (from panicle primordial initiation to spikelet initiation) contributes to the differentiation of branches and spikelets. The N absorbed during the late phase of panicle formation increases the hull size and percentage of filled grains by decreasing the number of degenerated spikelet, and contributes to grain filling by increasing specific leaf weight and N content in leaves. During the grain filling stage, N uptake is still required for the maintenance of the photosynthetic capacity and the promotion of carbohydrate accumulation in grains, which in turn affects the 1000-grain weight.

Other than nitrogen, incident solar radiation and temperature may also affect the grain yield, particularly during the reproductive and ripening stages (Yoshida and Parao 1976; De Datta 1981). However, the possibility of an uneven distribution of incident solar radiation and temperature could be excluded given the small size of the study site and the lack of any apparent clustering of yield classes. Therefore, an inadequate N supply may be the main cause of low yield.

However, N fertilizers were applied excessively in the study area (206 kg N ha^{-1} vs. the local recommendation of 140 kg N ha^{-1}), with about 1/4 applied as a basal treatment at the field preparation stage and the remaining 3/4 applied as a top dressing in three or five portions between transplanting and heading. Chlorophyll meter readings taken shortly before heading were higher than 37 in all yield classes, which is a critical value for N

deficiency in rice plants according to Balasubramanian et al. (2000) and Singh et al. (2002). It follows that there were no significant differences in chlorophyll meter readings among yield classes (Table 6). No measurements were made of the leaching rates and soluble soil N content during the early season. However, judging from the different soil properties among the yield classes, as discussed above, we suspect that a significant amount of pre-planting applied N may have been lost through leaching, leading to insufficient N for the development of more tillers during the vegetative growth stage in the low yielding areas. The differentiation of branches and spikelets might also have been affected during the early phase of panicle formation. Therefore, the aerial spikelet density was less in the low yielding areas. The frequent top dressing of N fertilizers before heading explained why N deficiencies were not detected by the chlorophyll meter. Only slight and inconsistent differences in 1000-grain weight values were observed between the yield classes.

Conclusion

Satellite-based yield estimates revealed year/crop season differences for paddy-rice grown at the study site in Taiwan. Remotely sensed yield classes helped to determine the appropriate locations for soil and plant sampling. The systematic approach developed in this study might potentially be applied to the identification and characterization of yield limiting factors in other paddy-rice growing areas, because the requisite year/crop season yield maps can be retrieved from historical satellite images.

Reduced grain yield in low-yielding areas is attributed to apparent early-season leaching loss of the basal N fertilizer application, which then significantly reduced the aerial spikelet density. However, more direct and statistically significant evidence, such as the early season leaching loss of applied N fertilizers, is still required to validate our hypothesis. Given that the in-season N application rates were somewhat higher than the local recommendations, we suggest reducing the amount of basal N applied because it could be lost, but applying the first top dressing shortly after transplantation to encourage panicle and spikelet development. Application of slow release forms of N fertilizers should be considered to reduce the potential contamination of downstream water resources.

References

Aparicio, N., Villegas, D., Casadesus, J., Araus, J. L., & Royo, C. (2000). Spectral vegetation indices as nondestructive tools for determining durum wheat yield. *Agronomy Journal, 92*, 83–91.

Balasubramanian, V., Morales, A. C., Cruz, R. T., Thiyagarajan, T. M., Nagarajan, R., Babu, M., et al. (2000). Adaptation of the chlorophyll meter (SPAD) technology for real-time N management in rice: A review. *International Rice Research Institute, 5*, 25–26.

Birrell, S. J., Sudduth, K. A., & Borgelt, S. C. (1993). Crop yield mapping using GPS. ASAE Paper MC93-104. ASAE, St. Joseph, MI.

Blackmer, T. M., Schepers, J. S., Varvel, G. E., & Walter-Shea, E. A. (1996). Nitrogen deficiency detection using reflected shortwave radiation from irrigated crop canopies. *Agronomy Journal, 88*, 1–5.

Blackmore, S. (2000). The interpretation of trends from multiple yield maps. *Computers and Electronics in Agriculture, 26*, 37–51.

Boydell, B., & McBratney, A. B. (2002). Identifying potential within-field management zones from cotton-yield estimates. *Precision Agriculture, 3*, 9–23.

Broge, N. H., & Leblanc, E. (2000). Comparing prediction power and stability of broadband and hyper-spectral vegetation indices for estimation of green leaf area index and canopy chlorophyll density. *Remote Sensing of Environment, 76*, 156–172.

Carr, P. M., Carlson, G. R., Jacobsen, J. S., Nielsen, G. A., & Skogley, E. O. (1991). Farming soils, not fields: A strategy for increasing fertilizer profitability. *Journal of Production Agriculture, 4*, 57–61.

Cassman, K. G., Dobermann, A., & Walters, D. T. (2002). Agroecosystems, nitrogen-use efficiency, and nitrogen management. *Ambio, 31*, 132–140.

Chang, K. W., Shen, Y., & Lo, J. C. (2005). Predicting rice yield using canopy reflectance measured at booting stage. *Agronomy Journal, 97*, 872–878.

Cox, M. S., & Gerard, P. D. (2007). Soil management zone determination by yield stability analysis and classification. *Agronomy Journal, 99*, 1357–1365.

De Datta, S. K. (1981). *Principles and practices of rice production*. Wiley.

Dobermann, A., Ping, J. L., Adamchuk, V. I., Simbahan, G. C., & Ferguson, R. B. (2003). Classification of crop yield variability in irrigated production fields. *Agronomy Journal, 95*, 1105–1120.

Ferguson, R. B., Hergert, G. W., Schepers, J. S., Gotway, C. A., Cahoon, J. E., & Peterson, T. A. (2002). Site-specific nitrogen management of irrigated maize: Yield and soil residual nitrate effects. *Soil Science Society of America Journal, 66*, 544–553.

Fleming, K. L., Heermann, D. F., & Westfall, D. G. (2004). Evaluating soil color with farmer input and apparent soil electrical conductivity for management zone delineation. *Agronomy Journal, 96*, 1581–1587.

Fleming, K. L., Westfall, D. G., Wiens, D. W., & Brodah, M. C. (2000). Evaluating farmer developed management zone maps for variable rate fertilizer application. *Precision Agriculture, 2*, 201–215.

Fraisse, C. W., Sudduth, K. A., & Kitchen, N. R. (2001). Delineation of site-specific management zones by unsupervised classification of topographic attributes and soil electrical conductivity. *Transactions of the ASAE, 44*, 155–166.

Franzen, D. W., Halvorson, A. D., & Hoffman, V. L. (2000). Management zones for soil N and P levels in the Northern Great Plains. In: P. C. Robert et al. (Eds.), *Proceedings of 5th international conference on precision agriculture, Minneapolis, MN [CD-ROM]. 16–19 July 2000*. ASA, CSSA, and SSSA, Madison, WI.

Franzen, D. W., & Nanna, T. N. (2002). Management zone delineation methods. In P. C. Robert et al. (Eds.), *Proceedings of 6th International conference on precision agriculture, Minneapolis*, MN *[CD-ROM]. 14–17 July 2002* (pp. 363–377). ASA, CSSA, and SSSA, Madison, WI.

Frazier, B. E., Walters, C. S., & Perry, E. M. (1997). Role of remote sensing in site-specific management. In F. J. Pierce & E. J. Sadler (Eds.), *The state of site-specific management for agriculture* (pp. 149–160). CSSA, SSSA, Madison, WI: ASA.

Guyot, G. (1990). Optical properties of vegetation canopies. In M. D. Steven & J. A. Clark (Eds.), *Applications of remote sensing in agriculture* (pp. 19–43). London: Butterworths.

Hansen, P. M., & Schjoerring, J. K. (2003). Reflectance measurement of canopy biomass and nitrogen status in wheat crops using normalized difference vegetation indices and partial least squares regression. *Remote Sensing of Environment, 86*, 542–553.

Hatfield, J. L., Gitelson, A. A., Schepers, J. S., & Walthall, C. L. (2008). Application of spectral remote sensing for agronomic decisions. *Agronomy Journal, 100*, S117–S131.

Hong, N., White, J. G., Weisz, R., Crozier, C. R., Gumpertz, M. L., & Cassel, D. K. (2006). Remote sensing-informed variable-rate nitrogen management of wheat and corn: Agronomic and groundwater outcomes. *Agronomy Journal, 98*, 327–338.

Hsieh, S. C., & Liu, D. J. (Eds.). (1979). The causes of low yield of the second crop rice in Taiwan and the measures for improvement (in Chinese). In *Proceedings of a symposium held at Taiwan Agricultural Research Institute*, June 7–8, 1978. Taiwan, ROC: National Science Council.

Jaynes, D. B., & Colvin, T. S. (1997). Spatiotemporal variability of corn and soybean yield. *Agronomy Journal, 89*, 30–37.

Kitchen, N. R., Drummond, S. T., Lund, E. D., Sudduth, K. A., & Buchleiter, G. W. (2003). Soil electrical conductivity and topography related to yield for three contrasting soil-crop systems. *Agronomy Journal, 95*, 483–495.

Klute, A. (Ed.). (1986). *Methods of soil analysis. Part 1. Physical and mineralogical methods*. ASA, CSSA, SSSA.

Lamb, J. A., Dowdy, R. H., Anderson, J. L., & Rehm, G. W. (1997). Spatial and temporal stability of corn grain yields. *Journal of Production Agriculture, 10*, 410–414.

Link, J., Graeff, S., Batchelor, W. D., & Claupein, W. (2006). Spatial variability and temporal stability of corn (*Zea mays* L.) grain yields—Relevance of grid size. *Archives of Agronomy and Soil Science, 52*, 427–439.

Machado, S., Bynum, E. D., Archer, T. L, Jr., Lascano, R. J., Wilson, L. T., Bordovsky, J., et al. (2002). Spatial and temporal variability of corn growth and grain yield: Implications for site-specific farming. *Crop Science, 42*, 1564–1576.

Mae, T. (1997). Physiological nitrogen efficiency in rice: Nitrogen utilization, photosynthesis, and yield potential. *Plant and Soil, 196*, 201–210.

McBratney, A. B., Whelan, B. M., Taylor, J. A., & Pringle, M. J. (2000). A management opportunity index for precision agriculture. In: P. C. Robert et al. (Eds.), *Proceedings of 5th international conference on precision agriculture, Minneapolis, MN [CD-ROM]*. 16–19 July 2000. ASA, CSSA, and SSSA, Madison, WI.

Mulla, D. J., & Schepers, J. S. (1997). Key processes and properties for site-specific soil and crop management. In F. J. Pierce & E. J. Sadler (Eds.), *The state of site-specific management for agriculture* (pp. 1–18). CSSA, SSSA, Madison, WI: ASA.

Pierce, F. J., Anderson, N. W., Colvin, T. S., Schueller, J. K., Humburg, D. S., & McLauglin, N. B. (1997). Yield mapping. In F. J. Pierce & E. J. Sadler (Eds.), *The state of site-specific management for agriculture* (pp. 211–244). CSSA, SSSA, Madison, WI: ASA.

Powers, J. F., Wiese, R., & Flowerday, D. (2000). Managing nitrogen for water quality—Lessons from management system evaluation. *Journal of Environmental Quality, 29*, 355–366.

Schepers, A. R., Shanahan, J. F., Liebig, M. A., Schepers, J. S., Johnson, S. H., & Luchiari, A, Jr. (2004). Appropriateness of management zones for characterizing spatial variability of soil properties and irrigated corn yields across years. *Agronomy Journal, 96*, 195–203.

Singh, B., Singh, Y., Ladha, J. K., Bronson, K. F., Balasubramanian, V., Singh, J., et al. (2002). Chlorophyll meter—and leaf color chart-based nitrogen management for rice and wheat in northwestern India. *Agronomy Journal, 94*, 821–829.

Sparks, D. L. (Ed.). (1996). *Methods of soil analysis. Part 3. Chemical methods*. ASA, CSSA, SSSA.

Steinwand, A. L., Karlen, D. L., & Fenton, T. E. (1996). An evaluation of soil survey crop yield interpretations for two central Iowa farms. *Journal of Soil and Water Conservation, 51*, 66–71.

Thenkabail, P. S. (2002). Optimal hyperspectral narrowbands for discriminating agricultural crops. *Remote Sensing Reviews, 20*(4), 257–291.

Thenkabail, P. S., Smith, R. B., & De Pauw, E. (2000). Hyperspectral vegetation indices and their relationships with agricultural crops. *Remote Sensing of Environment, 71*, 158–182.

Tiffany, D. G., Foord, K., & Eidman, V. (2000). Grower paths to profitable usage of precision agriculture technologies. In: Robert, P. C., et al. (Eds.), *Proceedings of 5th international conference on precision agriculture, Minneapolis, MN [CD-ROM]*. 16–19 July 2000. ASA, CSSA, and SSSA, Madison, WI.

Wang, Y. P., Chang, K. W., Chen, R. K., Lo, J. C., & Shen, Y. (2010). Large area rice yield forecasting using satellite imageries. *International Journal of Applied Earth Observation and Geoinformation, 12*, 27–35.

Wiegand, C. L., Richardson, D. E., Escobar, D. E., & Everitt, J. H. (1994). Photographic and video graphic observations for determining and mapping the response of cotton to soil salinity. *Remote Sensing of Environment, 49*, 212–223.

Wollenhaupt, N. C., Mulla, D. J., & Gotway Crawford, C. A. (1997). Soil sampling and interpolation techniques for mapping spatial variability of soil properties. In Pierce, F. J., & Sadler, E. J. (Eds.), *The state of site specific management for agriculture* (pp. 19–53). ASA, CSSA, and SSSAJ, Madison, WI.

Yoshida, S. (1981). *Fundamentals of rice crop science*. Los Baños, Philippines: IRRI.

Yoshida, S., & Parao, F. T. (1976). Climatic influence on yield and yield components of lowland rice in the tropics. In: *Climate and rice* (pp. 471–494). Los Baños, Philippines: IRRI.